Electronic Supplementary Material (ESI) for Materials Horizons.


# Supplementary Information

## Constructing asymmetric gradient structure to enhance energy storage performance of PEI-based composite dielectrics

Dong Yue,[ab] Wenchao Zhang,*[ab] Puzhen Wang,[ab] Yong Zhang,[ab] Yu Teng,[ab] Jinghua Yin,[ab] Yu Feng*[ab]

[a] Key Laboratory of Engineering Dielectrics and Its Application, Ministry of Education, Harbin University of Science and Technology, Harbin 150080, P. R. China

[b] School of Electrical and Electronic Engineering, Harbin University of Science and Technology, Harbin 150080, P. R. China

**Stochastic breakdown Model**

In the stochastic breakdown model, the breakdown probability *P*(r) is written as

$$P(r) = \frac{E(r)^2}{E_b(r)^2} \Big/ \sum \frac{E(r)^2}{E_b(r)^2} \tag{1}$$

where *E*(r) is the electric field of a local point determined by the externally applied voltage and the microstructure, and $E_b$(r) is the corresponding intrinsic breakdown strength determined by the polymer-based composite dielectrics, and the summation in the denominator is the sum over all points that the local electric field exceeds the breakdown strength.

The local electric field distribution is obtained by solving the electrostatic equilibrium equation using an spectral iterative perturbation method.[1] As we assume there exist no spontaneous polarization in the system and the relative permittivity is independent of the applied field strength, the electric displacement *D*(r,E) can be expressed using Einstein notation as

$$D_i(r,E) = \varepsilon_0 k_{ij}(r) E_j(r) \tag{2}$$

where *k*(r) is the relative dielectric constant of the composite material.

According to Gauss's law the gradient of the electric displacement equals the position-dependent free charge density, i.e.

$$\frac{\partial D_i(r,E)}{\partial x_i} = \frac{\partial \left[\varepsilon_0 k_{ij}(r) E_j(r)\right]}{\partial x_i} = \rho_f(r) \tag{3}$$

We know that total electric field equals to external field, $E^{ext}$, plus the depolarization field $E^d$,

$$E_j^d(r) = -\frac{\partial \varphi(r)}{\partial x_j} \tag{4}$$

where $\varphi$(r) is the "depolarization potential". Using this substitution, Eq. 3 becomes

$$\frac{\partial \left[ \varepsilon_0 k_{ij}(r)(E_j^{ext} - \frac{\partial \varphi(r)}{\partial x_j}) \right]}{\partial x_i} = \rho_f(r) \tag{5}$$

We can express the inhomogeneous relative dielectric constant as the sum of the homogeneous reference $k^0_{ij}$ and a perturbation $\Delta k_{ij}(r)$, i.e.

$$k_{ij}(r) = k_{ij}^0 + \Delta k_{ij}(r) \tag{6}$$

After substituting Eq. 6 into Eq. 5 and rearranging we obtain

$$k_{ij}^0 \frac{\partial^2 \varphi(r)}{\partial x_i \partial x_j} = \frac{\partial}{\partial x_i}\left[\Delta k_{ij}(r)(E_j^{ext} - \frac{\partial \varphi(r)}{\partial x_j})\right] - \frac{\rho_f(r)}{\varepsilon_0} \tag{7}$$

From which we can solve for the depolarization potential and thus the electric field. Details of the numerical method for solving this equation are described.

A grid size of $N_x\Delta x \times N_y\Delta x \times N_z\Delta x$ is employed in all simulations. For all simulations, $N_x = N_y = N_z = 128$. The relative permittivity of the breakdown phase $\varepsilon^B$ is considered to be isotropic and to have a value of $10^4$ to reflect its strong polarized ability due to the abundant space charge in the breakdown region. For each polymer-based composite dielectric, all fillers are generated with random distribution without overlapping. The materials parameters used in the simulation are listed in Table S1.

Table S1. Materials parameters used in the stochastic modeling of breakdown.

| Material | Dielectric constant | Breakdown strength (MV/m) |
|---|---|---|
| PEI | 3.5 | 400.5 |
| BNNS | 3 | 1000 |

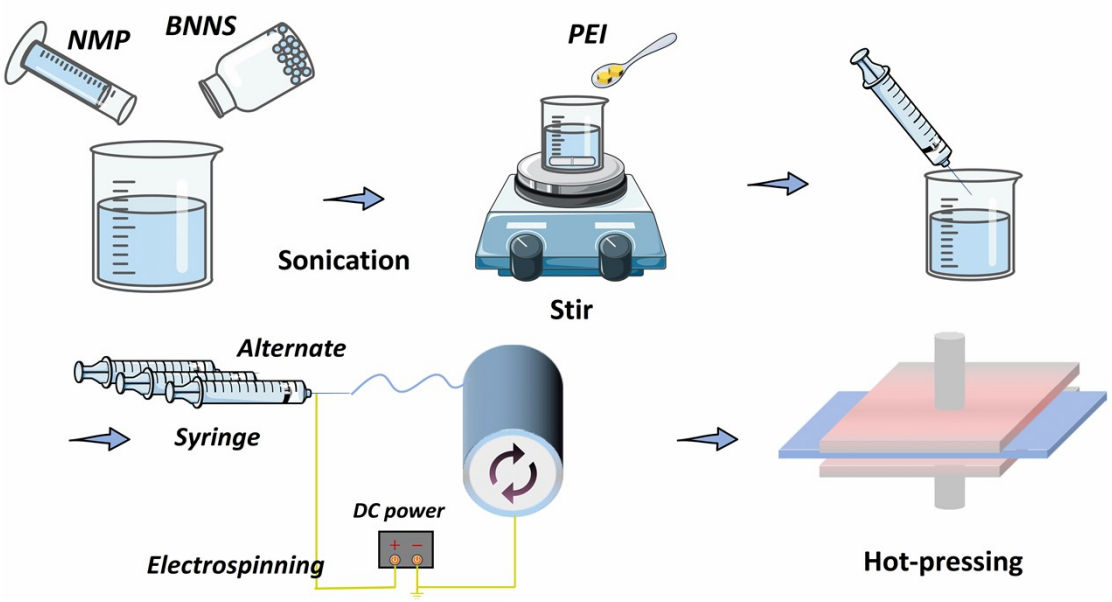


Fig. S1 Preparation schematic of PEI-based composite dielectrics

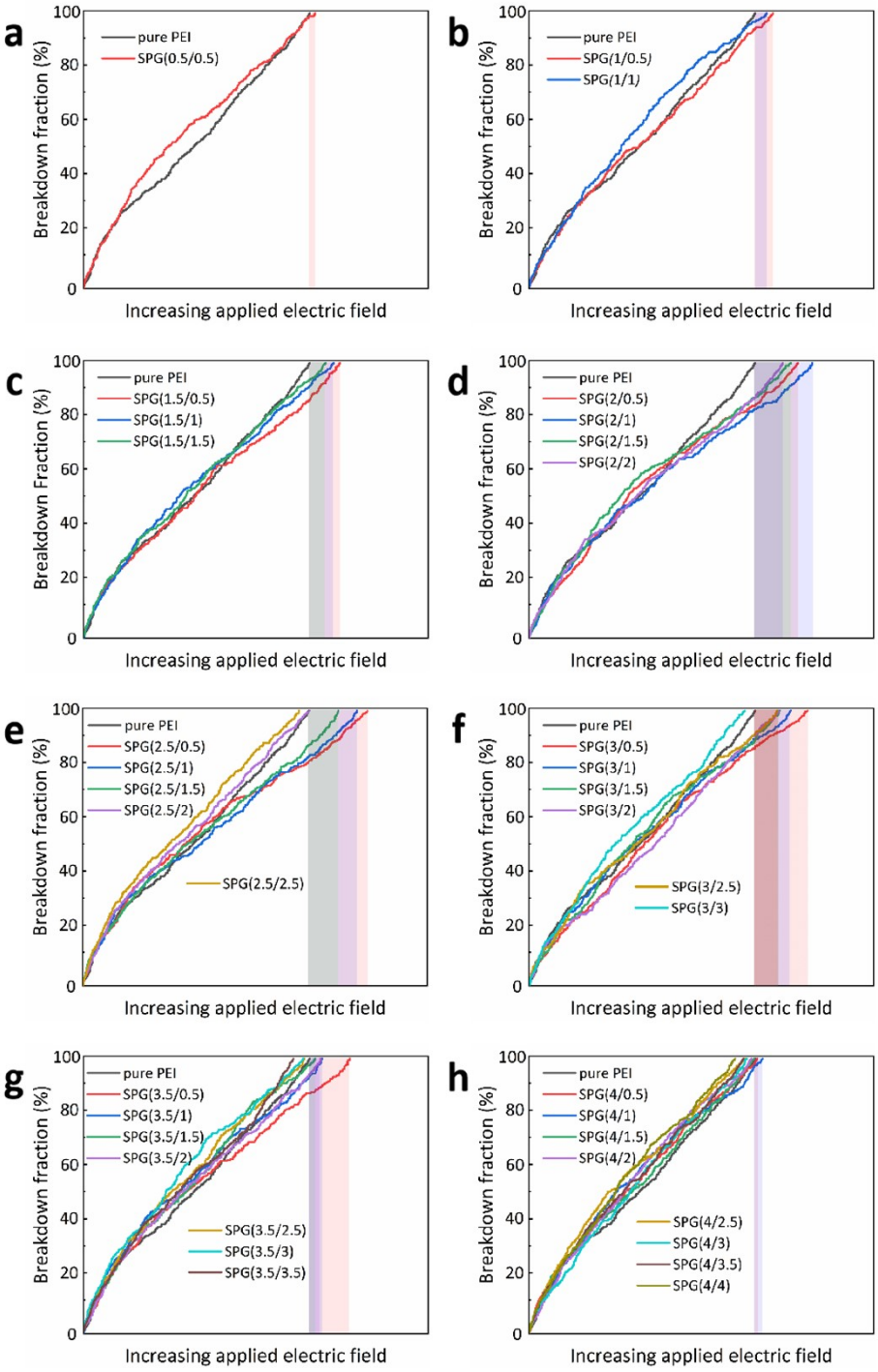


Fig. S2 Volume fraction of breakdown phase in SPG composite dielectrics

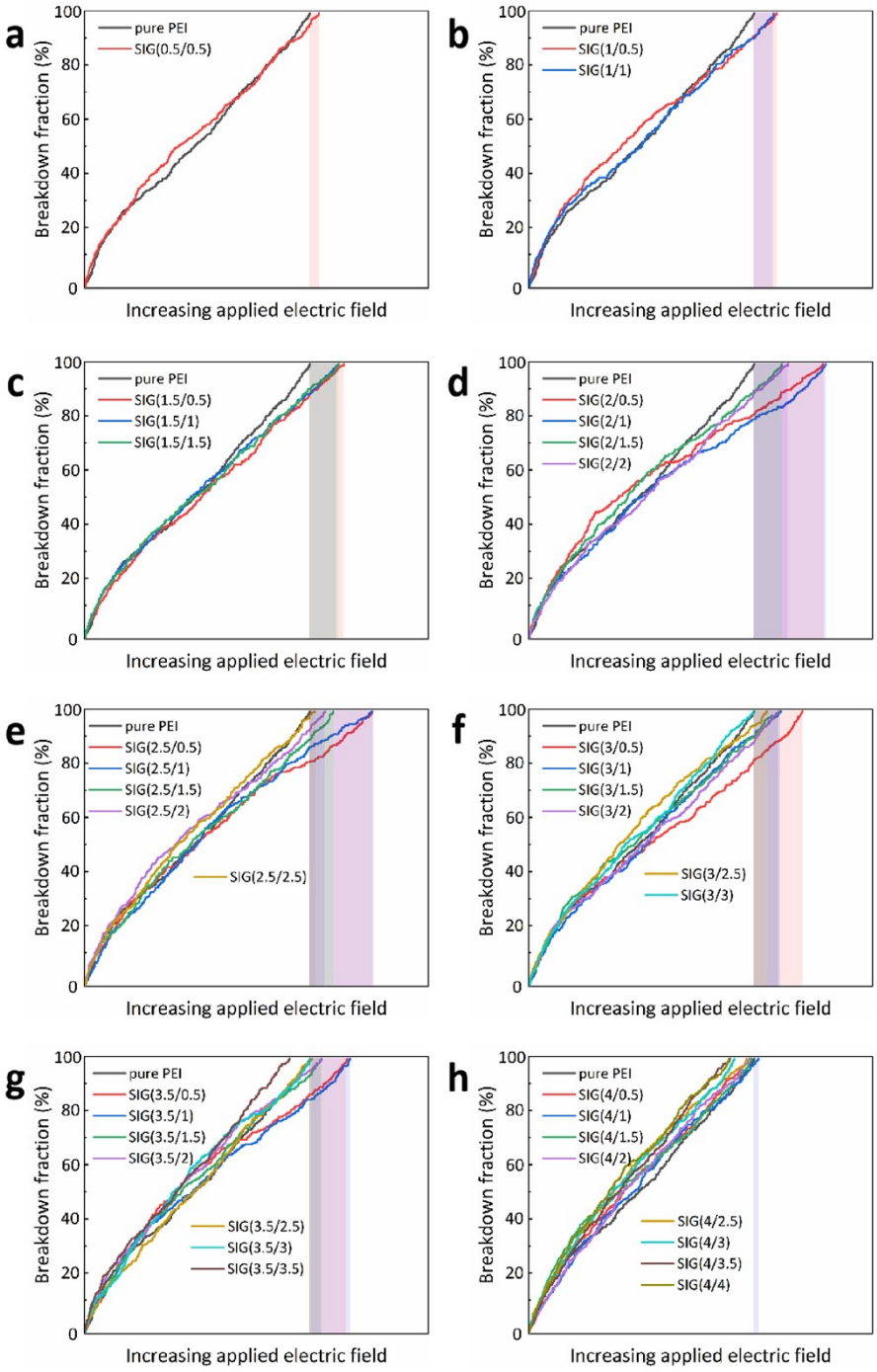


Fig. S3 Volume fraction of breakdown phase in SIG composite dielectrics

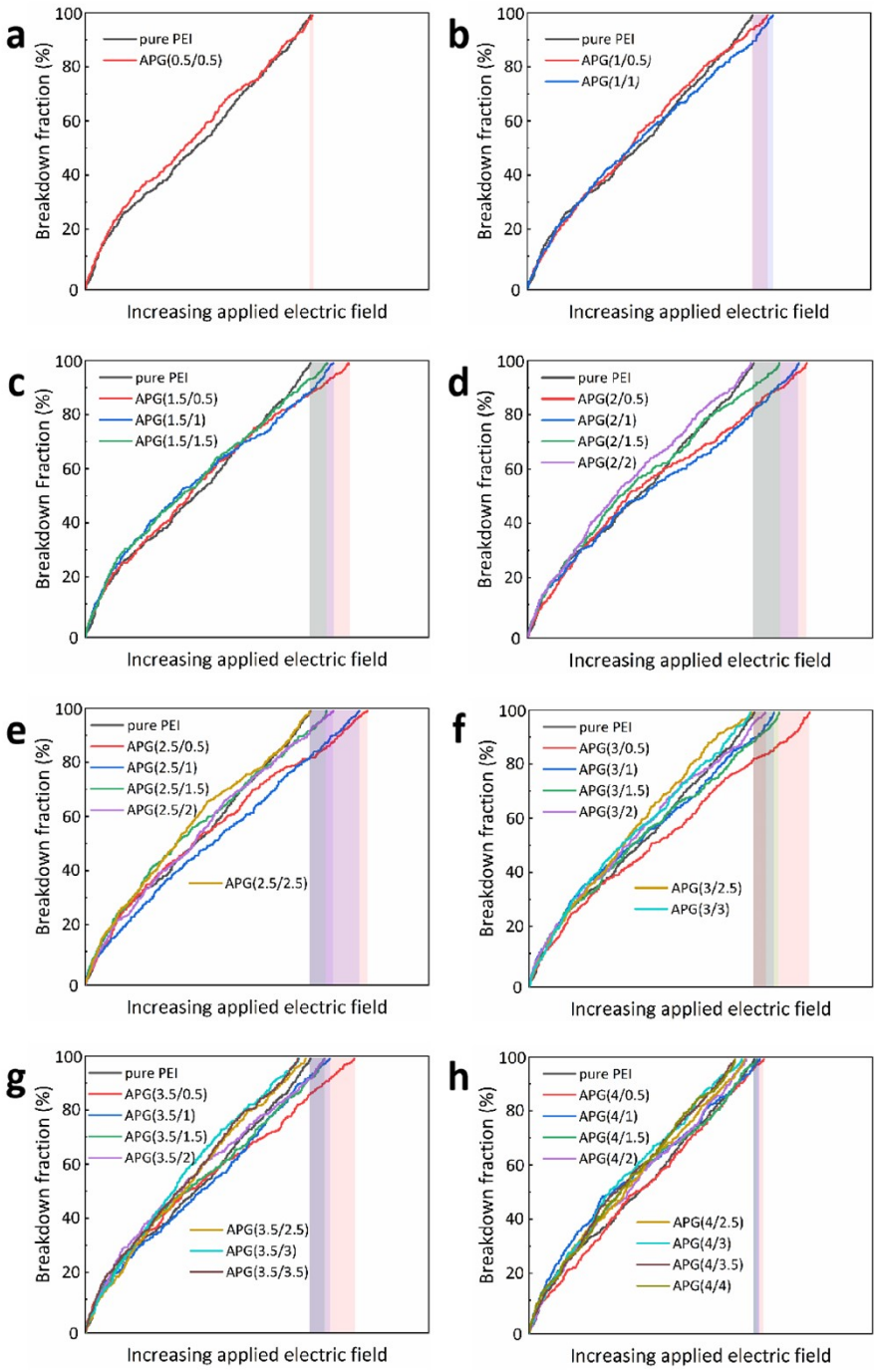


Fig. S4 Volume fraction of breakdown phase in APG composite dielectrics

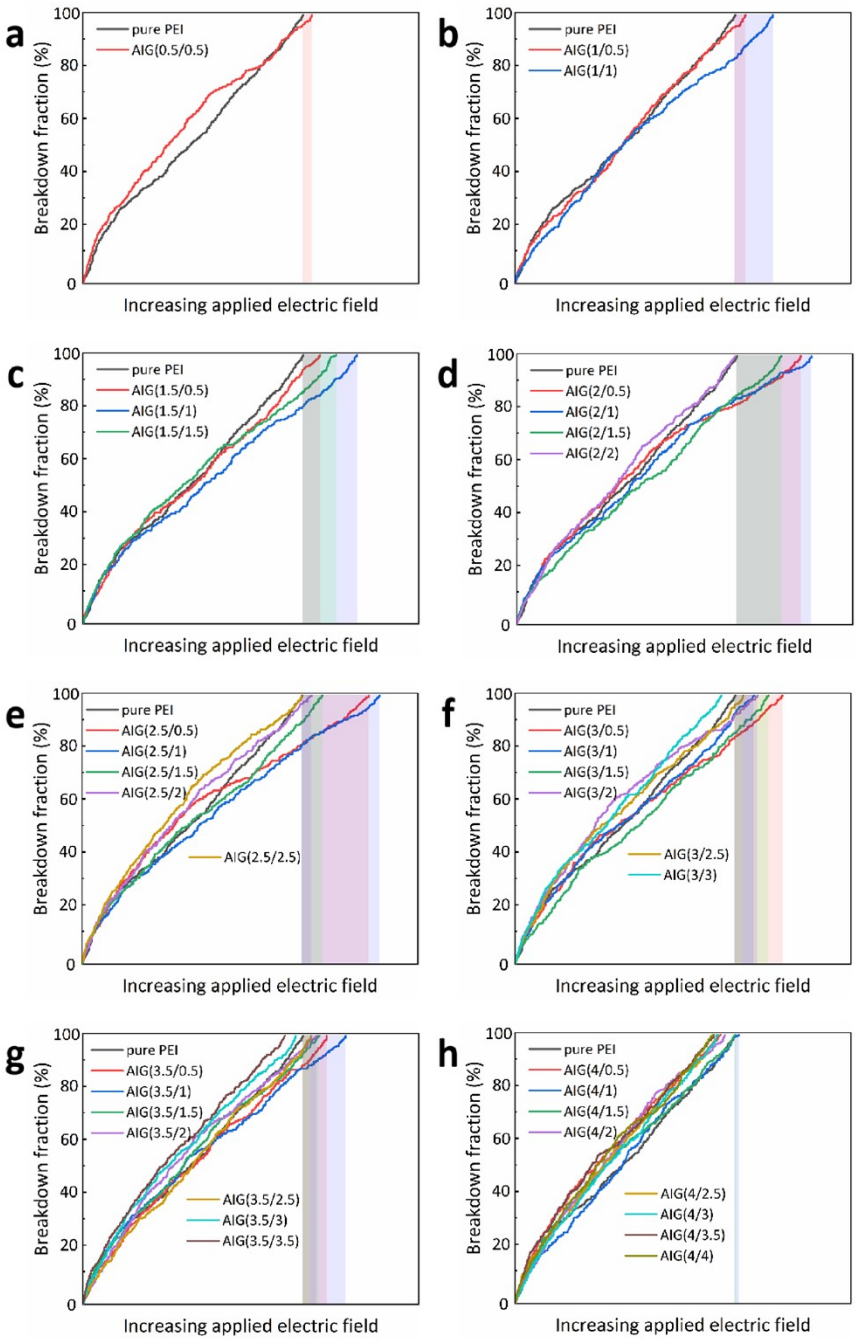


Fig. S5 Volume fraction of breakdown phase in AIG composite dielectrics

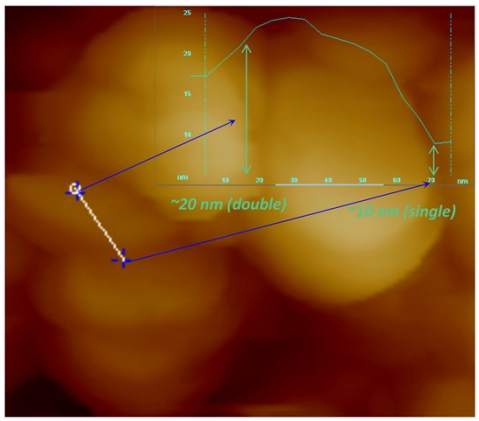


Fig. S6 AFM image of BNNS

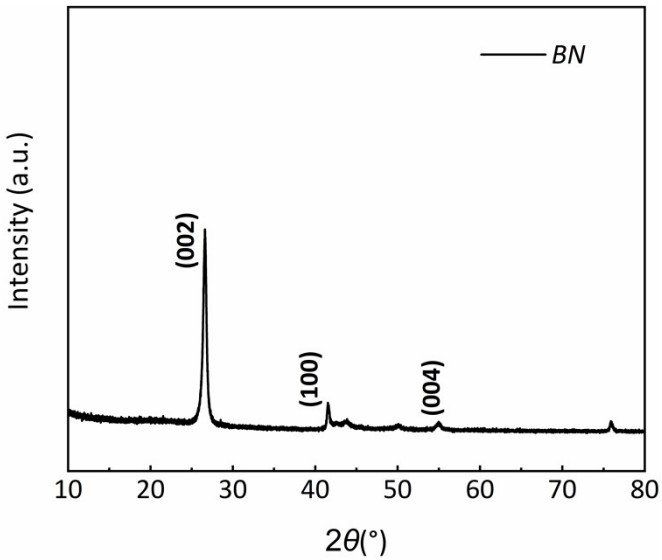


Fig. S7 XRD pattern of BNNS

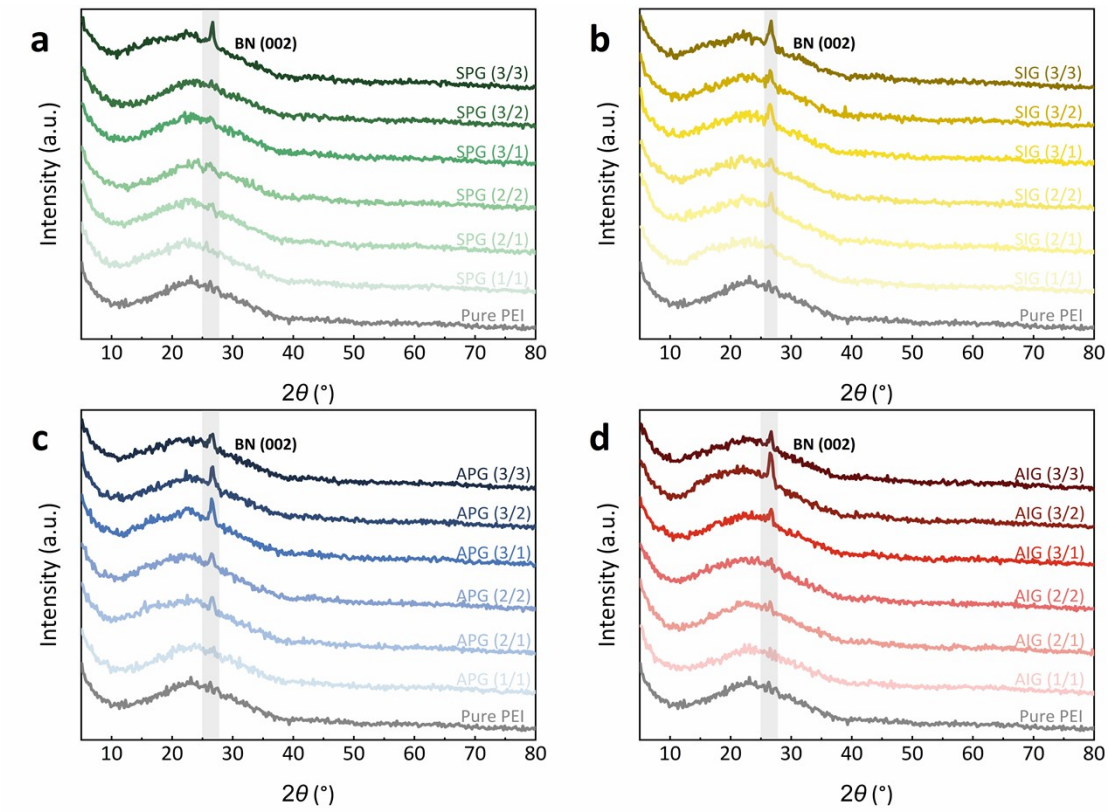


Fig. S8 XRD patterns of pure PEI and PEI-based composite dielectrics

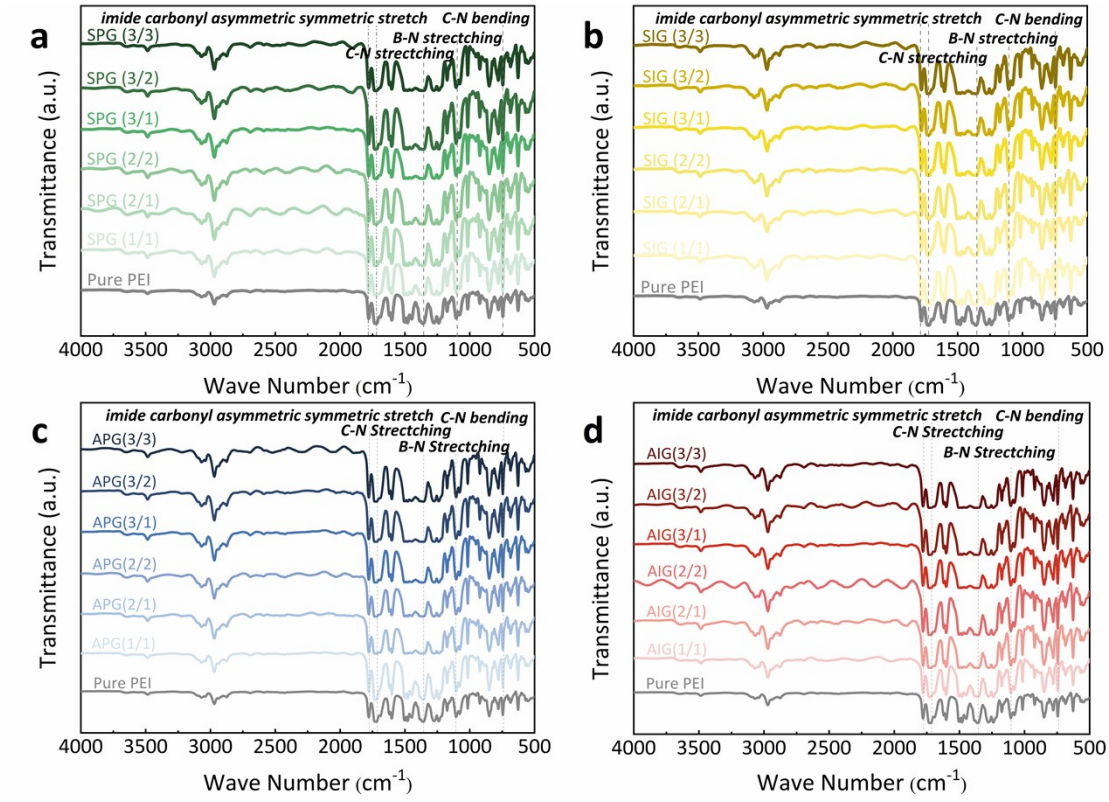


Fig. S9 FTIR spectra of pure PEI and PEI-based composite dielectrics

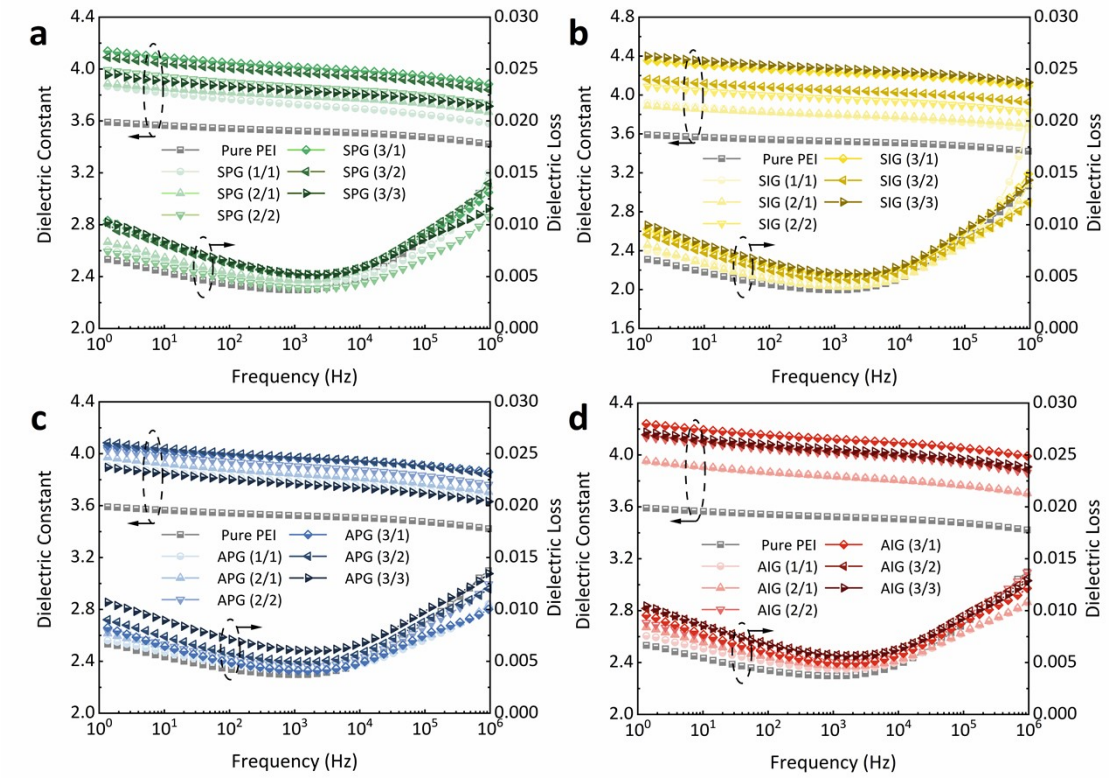


Fig. S10 The dielectric constant and dielectric loss of pure PEI and PEI-based composite dielectrics

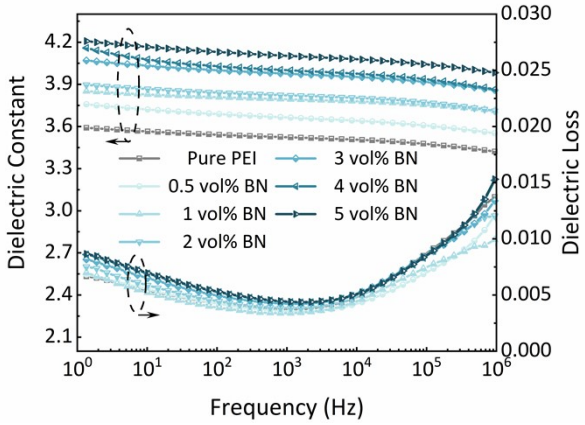


Fig. S11 The dielectric constant and dielectric loss of pure PEI and single-layer PEI-based composite dielectrics

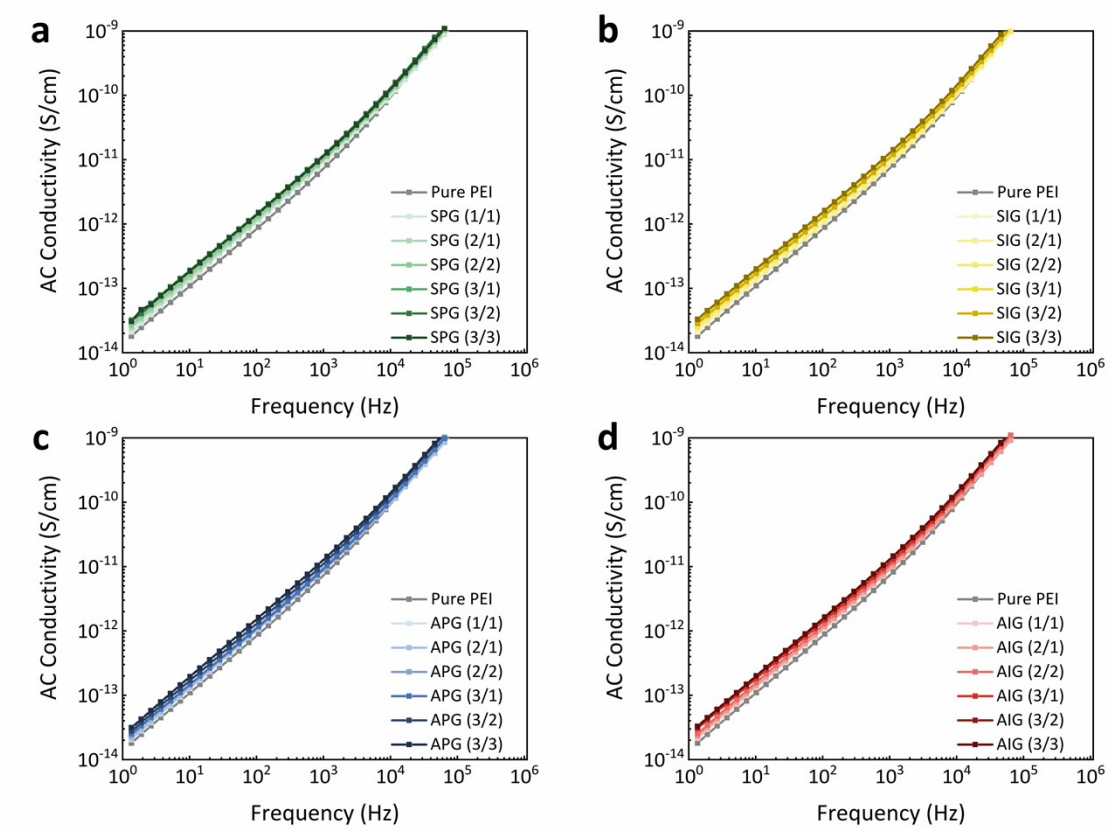


Fig. S12 The AC conductivity of pure PEI and PEI-based composite dielectrics

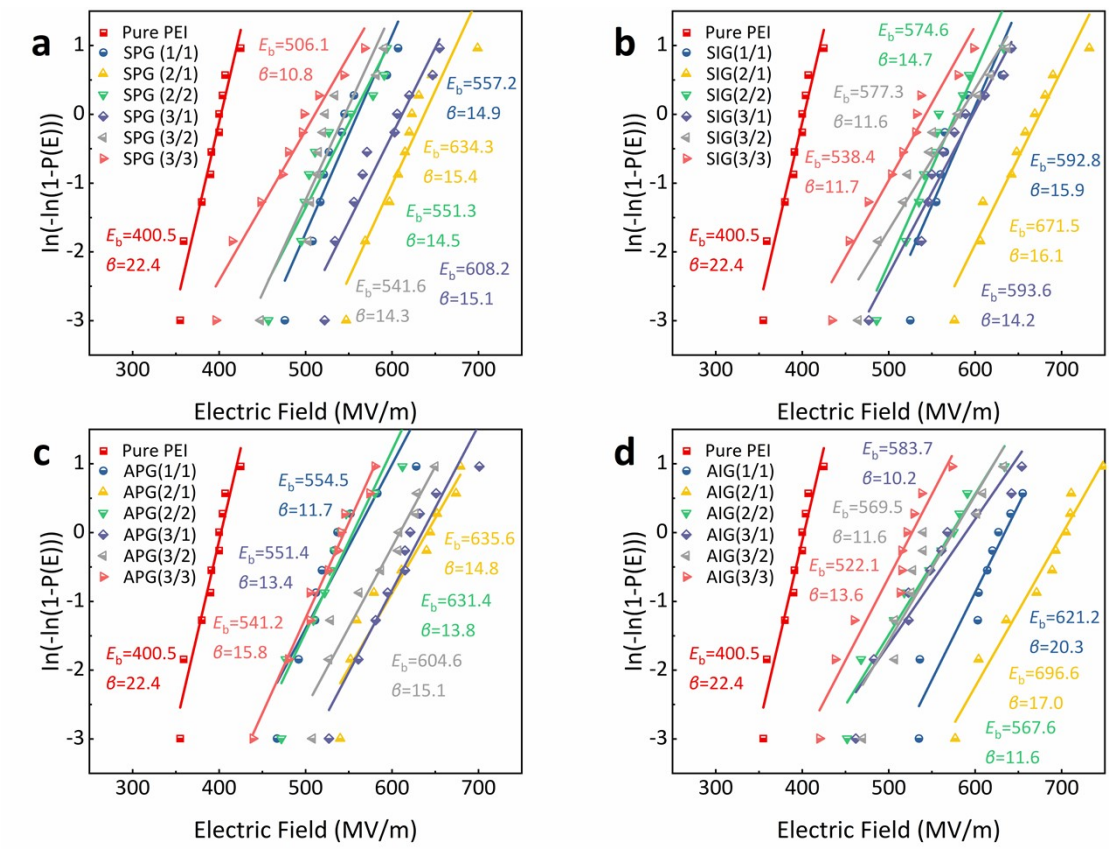


Fig. S13 The breakdown strength of pure PEI and PEI-based composite dielectrics

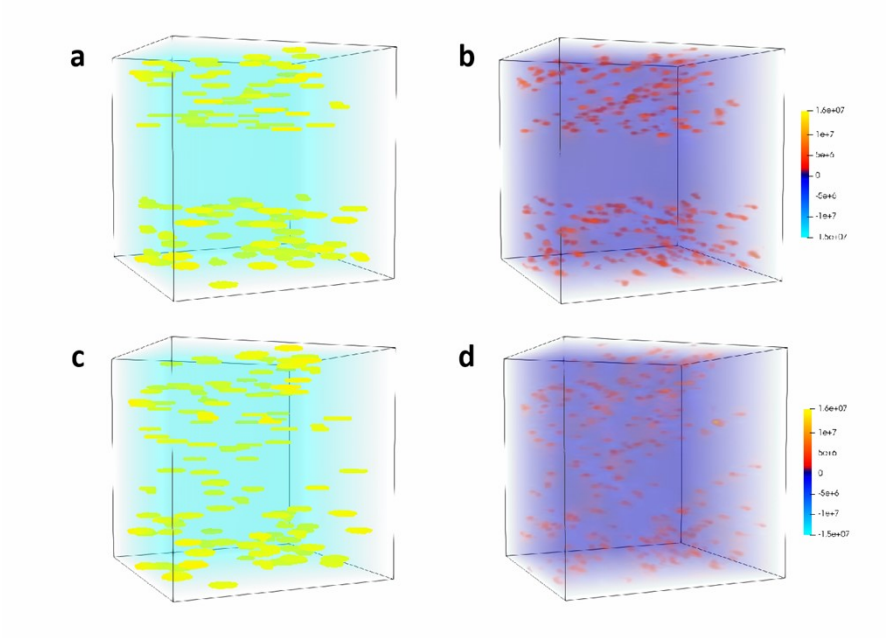


Fig. S14 a) Sandwich structure under no applied electric field. b) Electric field distribution simulation of sandwich structure under 200 MV/mm. c) Gradient structure under no applied electric field. d) Electric field distribution simulation of gradient structure under 200 MV/mm.

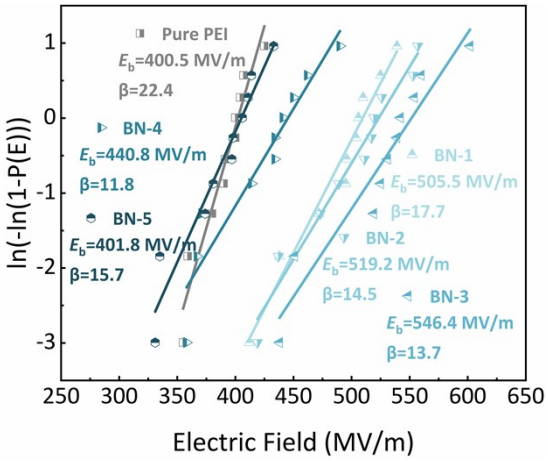


Fig. S15 The breakdown strength of pure PEI and single-layer PEI-based composite dielectrics

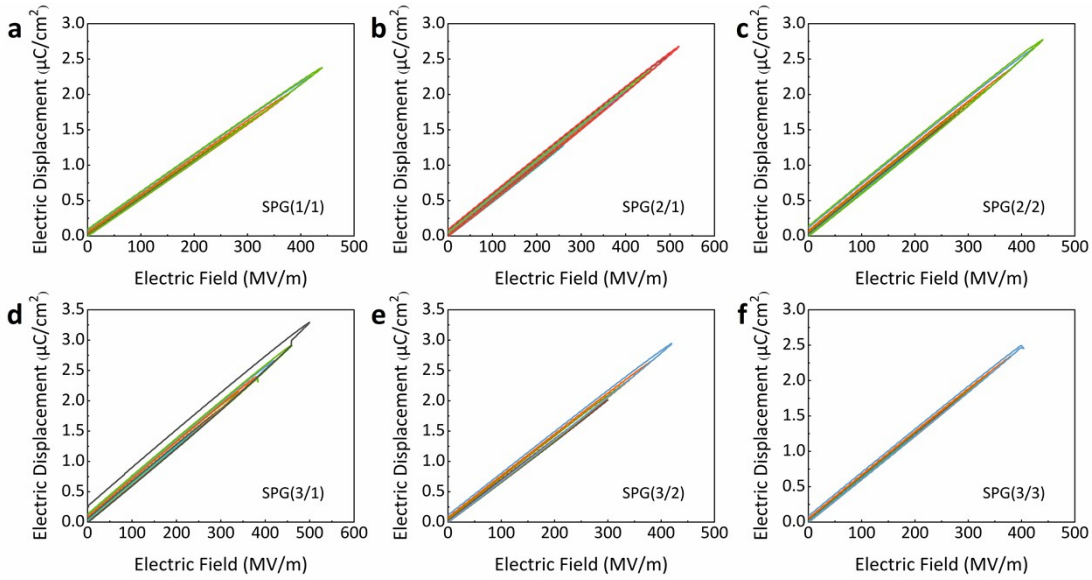


Fig. S16 The *D-E* loops of SPG composite dielectrics

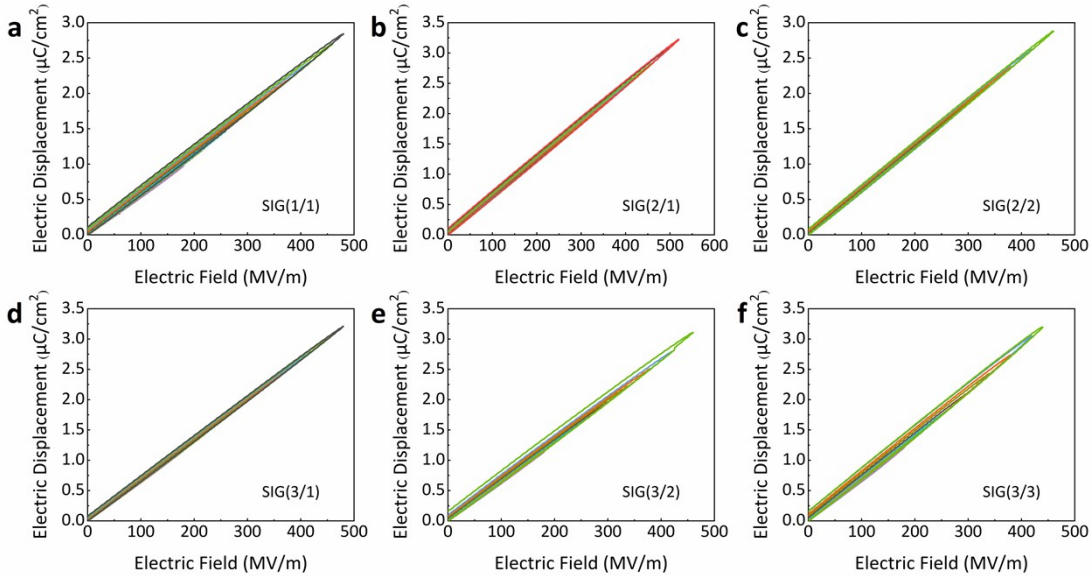


Fig. S17 The *D-E* loops of SIG composite dielectrics

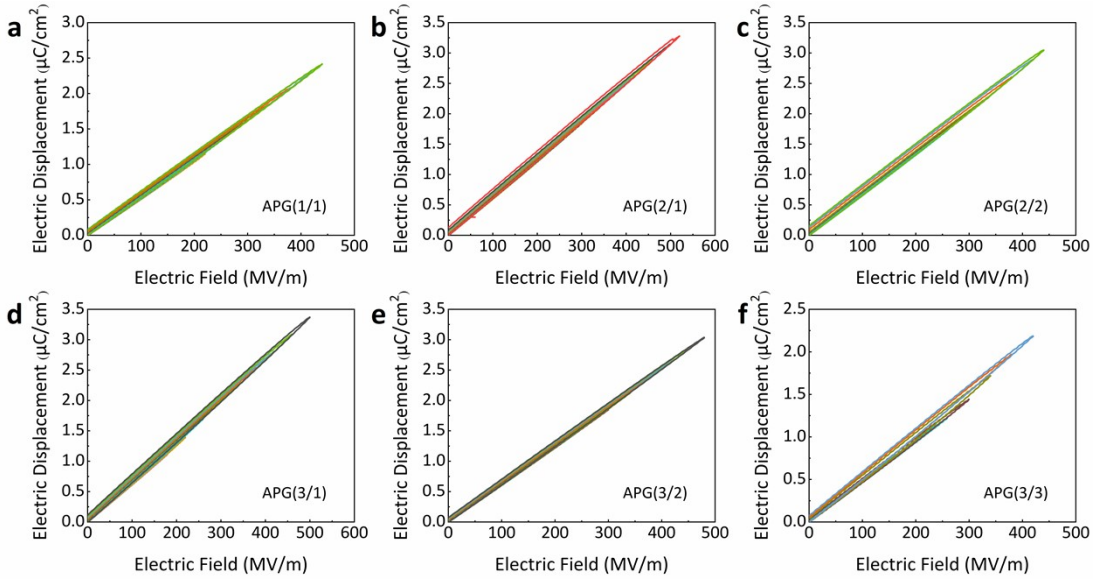


Fig. S18 The *D-E* loops of APG composite dielectrics

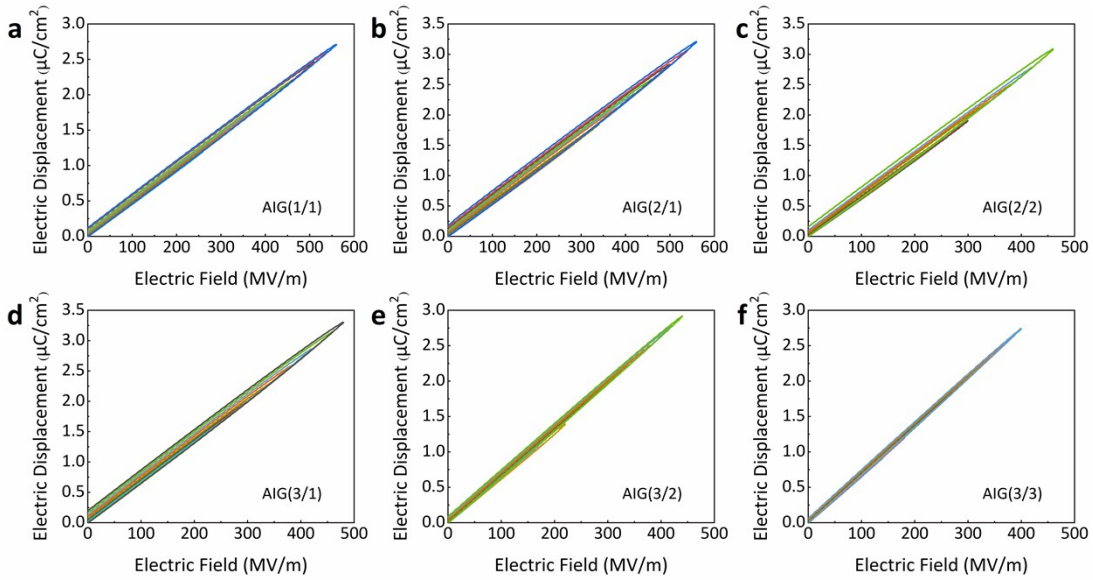


Fig. S19 The *D-E* loops of AIG composite dielectrics

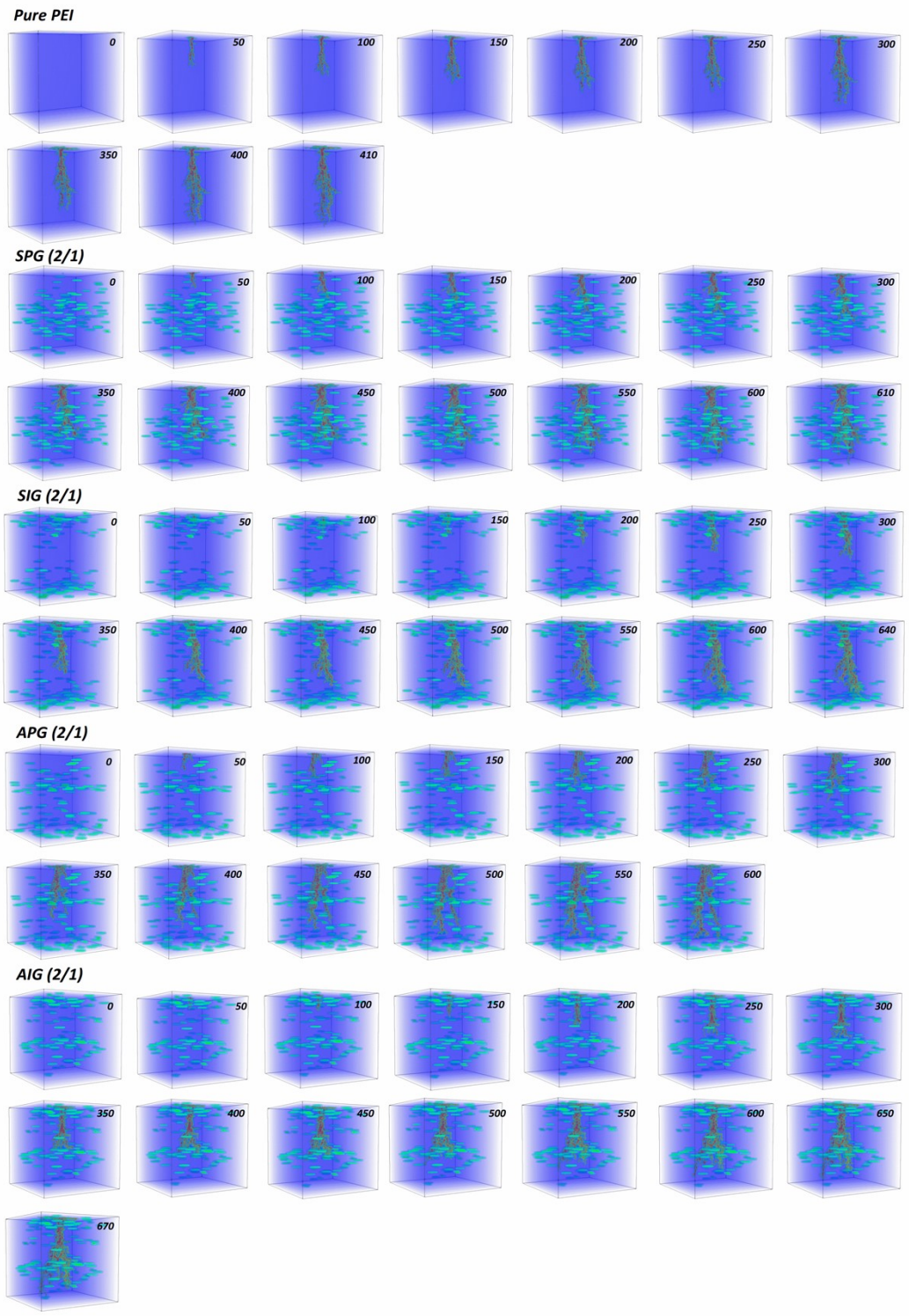


Fig. S20 Dynamic breakdown path development in pure PEI and PEI-based composite dielectrics

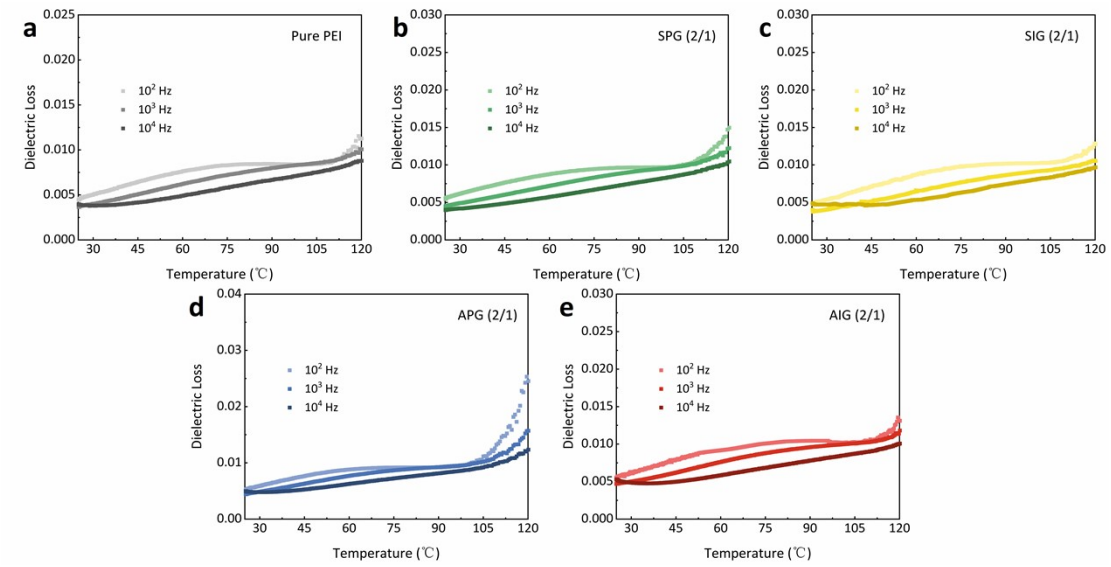


Fig. S21 The temperature dependence the dielectric loss of pure PEI and PEI-based composite dielectrics at $10^2$, $10^3$, $10^4$ Hz